Analysis for magnetic moment and electric dipole moment form factors of the top quark via $e^+e^- \to t\bar{t}$

D. Atwood and A. Soni
Department of Physics, Brookhaven National Laboratory, Upton, New York 11973
(Received 15 November 1991)

Phenomenological analysis for determining the magnetic moment and electic dipole moment form factors of the top quark via the reaction $e^+e^- \to t\bar{t}$, followed by the decays $t \to bW^+$ and $\bar{t} \to \bar{b}W^-$, is presented, with analytic expressions for the differential cross section and decay given. Various experimental observables are studied and their efficacy for the determination of form factors is considered and compared with the optimal resolution of form factors in the $t\bar{t}\gamma$ and $t\bar{t}Z$ vertices. We find that with a sample of 10 000 events it is possible to put limits of 10^{-18}–10^{-19} e cm for the form factors considered, evaluated at $q^2=s$ when $\sqrt{s} \approx 500$ GeV.

PACS number(s): 13.40.Fn, 13.10.+q, 14.80.Dq

I. INTRODUCTION

The fact that the top quark has not been discovered yet may eventually prove to be one of the most important physics nonevents of the 1980s. The current Collider Detector at Fermilab (CDF) limit [1] of 89 GeV puts the top-quark mass well into the electroweak scale, suggesting that top physics may be more sensitive to physics on the electroweak scale and beyond in a way that other quarks may not be. Experimental determination of the properties of the top quark will thus be an important priority in the coming decades (assuming that the top discovery is not too far in the future) and will perhaps be an important window on fundamental interactions beyond the standard model.

From the experimental point of view, the top quark also has the additional advantage that due to its large mass it may not hadronize. Thus, its decays may be directly observed in much the same way as in the case for a heavy lepton. In contrast, light quarks always appear in hadrons. Therefore, in order to put limits, for example, on the up- or down-quark electric dipole moment (EDM), it is necessary to consider the EDM of the neutron, making the theoretical interpretation very difficult.

Perhaps the cleanest method for measuring the properties of the top quark is to look at the pair-production reaction in e^+e^- colliders: $e^+e^- \to t\bar{t}$ followed by the subsequent weak decay of the top quarks, $t\bar{t} \to bW^+\bar{b}W^-$, where the W bosons decay leptonically, $W \to l\nu_l$ ($l=e$, μ, or τ). Such experiments may perhaps be possible at the CERN e^+e^- collider LEP II if the top-quark mass is very near the current limit, or otherwise at future e^+e^- colliders [2].

In this paper we consider $\gamma t\bar{t}$ and $Zt\bar{t}$ couplings and their effect on the differential cross section for the reaction $e^+e^- \to t\bar{t}$. The $\gamma t\bar{t}$ coupling consists of the standard-model tree-level ones as well as magnetic dipole moment (MDM) and electric dipole moment (EDM) couplings. Likewise, in addition to the tree-level standard-model $Zt\bar{t}$ coupling, we are including the analogous Z MDM and Z EDM couplings. In both cases we allow the possibility that these couplings may have imaginary parts. In our analysis, we assume for simplicity that the tbW vertex has the standard-model coupling.

The MDM-like couplings are present in the standard model at the one-loop level. On the other hand, the EDM-like couplings violate CP and, in fact, due to the structure of the standard model, are only present perturbatively in the standard model at three loops [3], although it could also arise nonperturbatively [4] through a nonzero value of $\theta_{\rm QCD}$. In some extensions to the standard model, however, EDM couplings may be present at lower order in perturbation theory [5]. Some models which can give relatively large fermion EDM's include left-right-symmetric theories, additional Higgs multiplets, supersymmetry, and composite models [5].

In order to observe these couplings, we consider in detail the distribution of the momenta of the final-state particles. For each of the couplings mentioned above, there are in general several possible observables which are sensitive to them. One may also construct an optimal observable which allows for the maximum sensitivity to the coupling in question. We have found examples for which the optimal observable does about one order of magnitude better in terms of sensitivity to the above couplings than observables which one might naively consider.

II. FORM OF INTERACTION

In this paper we will assume that the coupling between a fermion f and the boson V (where V represents either a γ, a Z boson, or possibly a Z' boson) takes the form

$$-i[\gamma^\mu(A_f^V+B_f^V\gamma_5)+\sigma^{\nu\mu}q_\nu(iC_f^V+D_f^V\gamma_5)] . \tag{1}$$

For the electron we assume that these parameters have their tree-level standard-model values; hence,

$$\begin{aligned} A_e^\gamma &= -e , \\ B_e^\gamma &= 0 , \\ A_e^Z &= \frac{e}{\sin\theta_W\cos\theta_W}(-\tfrac{1}{4}+\sin^2\theta_W) , \\ B_e^Z &= \frac{e}{4\sin\theta_W\cos\theta_W} , \end{aligned} \tag{2}$$

while $C_e^V = D_e^V = 0$. For the top quark, the tree-level standard-model values for these parameters are

$$A_t^\gamma = \tfrac{2}{3}e \ ,$$
$$B_t^\gamma = 0 \ ,$$
$$A_t^Z = \frac{e}{\sin\theta_W \cos\theta_W}\left(\tfrac{1}{4} - \tfrac{2}{3}\sin^2\theta_W\right) \ , \tag{3}$$
$$B_t^Z = -\frac{e}{4\sin\theta_W \cos\theta_W} \ ,$$
$$C_t^V = D_t^V = 0 \ .$$

The parameters C_t and D_t are the MDM and EDM form factors of the top quark evaluated at $q^2 = s$. In our calculations, we will expand the differential cross section to first order in these quantities. As mentioned above, throughout this paper we will assume that the Wtb coupling takes on the usual standard-model left-handed form.

In the Appendix, we calculate the differential cross section for $e^+e^- \to V \to t\bar{t}$, with subsequent $t\bar{t} \to W^+ b W^- \bar{b}$ as shown in the Feynman diagram in Fig. 1, where for simplicity we take $m_b = 0$. The expressions given are expanded to first order in C_t and D_t for both Z and γ exchange, including interference terms between the Z and γ graphs. Our calculation there has been done both in the case of unpolarized e^+e^- beams and e^+e^- beams of arbitrary polarization. The fact that the e^+e^- may be treated as massless allows for a straightforward generalization from the unpolarized to polarized case.

In our analysis we have also assumed that C_t and D_t may take on complex values which could arise from absorptive parts in the process which produces these effective couplings. Denoting the total differential cross section by $\Sigma(\phi)d\phi$, where ϕ represents the phase-space variables, we expand Σ to first order in C_t and D_t as

$$\Sigma = \Sigma_{AB} + \Sigma_{\mathrm{Re}(C)} + \Sigma_{\mathrm{Im}(C)} + \Sigma_{\mathrm{Re}(D)} + \Sigma_{\mathrm{Im}(D)} \ , \tag{4}$$

where Σ_{AB} depends only on A_t and B_t, $\Sigma_{\mathrm{Re}(C)}$ is linear in $\mathrm{Re}(C)$, $\Sigma_{\mathrm{Im}(C)}$ is linear in $\mathrm{Im}(C)$, $\Sigma_{\mathrm{Re}(D)}$ is linear in $\mathrm{Re}(D)$, and $\Sigma_{\mathrm{Im}(D)}$ is linear in $\mathrm{Im}(D)$.

Of course A_t, B_t, C_t, and D_t are in general s-dependent form factors. Since experimentally the e^+e^- collision takes place at a specific value of s, only the value of these form factors at the value of s will be accessible in a given experiment. Note that the explicit form of these terms given in the Appendix obeys the correct transformation properties under various discrete symmetries, as one would expect. For example, under CP, $\Sigma_{\mathrm{Re}(D)}$ and $\Sigma_{\mathrm{Im}(D)}$ are antisymmetric, while all $\Sigma_{\mathrm{Im}(C)}$ and $\Sigma_{\mathrm{Re}(C)}$ are symmetric. Also $\Sigma_{\mathrm{Re}(D)}$ and $\Sigma_{\mathrm{Im}(C)}$ are antisymmetric under T_n, where T_n denotes "naive" time reversal defined to be replacing t with $-t$ without switching initial and final states.

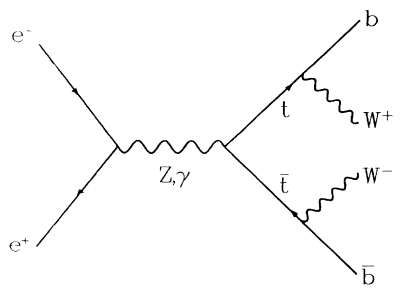

FIG. 1. Feynman diagrams for the process $e^+e^- \to t\bar{t} \to bW^+\bar{b}W^-$.

Experimentally, it is not possible to reverse the flow of time, so one cannot use T_n to experimentally distinguish between the real and imaginary couplings. In order to accomplish this, one needs a symmetry that is a symmetry of the domain of phase-space integration. Consider the transformation P_n, which we define to be parity applied to all boson polarizations and particle momenta while leaving fermion helicites fixed. P_n is clearly a transformation on the domain of integration, and by inspection of the expressions in the Appendix, all the Σ_i have identical symmetry properties under P_n and T_n. Thus, P_n can be used to experimentally differentiate between the real and imaginary parts of the couplings.

III. OPTIMIZED OBSERVABLE QUANTITIES

Before defining how to measure the EDM or MDM couplings, let us consider the general problem of observing the change in the differential cross section due to the addition of any small coupling. Here, we denote the differential cross section by

$$\Sigma(\phi)d\phi \ , \tag{5}$$

where ϕ represents the relevant phase-space variables being considered (including angular and polarization variables). Suppose now that there is a small contribution to this differential cross section controlled by a parameter λ (for example, λ could be the EDM or MDM) so that if we expand the total differential cross section in terms of λ we have

$$\Sigma = \Sigma_0 + \lambda\Sigma_1 \ . \tag{6}$$

If one has an ideal detector that records accurately the value of ϕ for each event that occurs, any method for determining the value of λ amounts to weighting the events with a phase-space-dependent function $f(\phi)$ and calculating the quantity

$$f^{(1)}(\lambda) = \int f(\phi)\Sigma(\phi)d\phi \ , \tag{7}$$

as compared to the value if $\lambda = 0$:

$$f^{(1)}(0) = \int f(\phi)\Sigma_0(\phi)d\phi \ . \tag{8}$$

Thus, the change due to the presence of λ is given by

$$\delta_f = f^{(1)}(\lambda) - f^{(1)}(0) = \lambda\int f(\phi)\Sigma_1(\phi)d\phi \ . \tag{9}$$

We must now compare δ_f with the error in measuring $f^{(1)}$. If n events are recorded, this error will be given by

$$\Delta f = \left[\frac{f^{(2)}\sigma}{n}\right]^{1/2} \ , \tag{10}$$

where $\sigma=\int\Sigma\,d\phi$ is the total cross section and $f^{(2)}=\int f^2\Sigma\,d\phi$. Let us now define the "resolving power" R of the function f in terms of the appropriately normalized ratio of these two quantities by

$$R=\frac{1}{n\lambda^2}\frac{\delta_f^2}{(\Delta f)^2}=\frac{[f^{(1)}(\lambda)-f^{(1)}(0)]^2}{\lambda^2 f^{(2)}\sigma}=\frac{\left[\int f(\phi)\Sigma_1(\phi)d\phi\right]^2}{\sigma\int f^2(\phi)\Sigma_0(\phi)d\phi}\ . \tag{11}$$

Thus, the statistical significance S with which the presence of a nonzero value of λ may be ascertained is

$$S=\frac{\delta_f}{\Delta f}=\lambda\sqrt{nR}\ . \tag{12}$$

The larger the value of R, therefore, the more effective f is for measuring λ, so that if at all possible, one would like to use a function f for which R is maximal.

In order to find such an optimal function, which we will denote $f_{\rm opt}$, it is useful to decompose an arbitrary function f as

$$f=A\frac{\Sigma_1}{\Sigma_0}+\hat{f}\ , \tag{13}$$

where we define the quantity

$$A=\frac{\int f\Sigma_1 d\phi}{\int\frac{\Sigma_1^2}{\Sigma_0}d\phi}\ . \tag{14}$$

Therefore, $\hat{f}$ defined by Eq. (13) has the property that $\int\hat{f}\Sigma_1 d\phi=0$.

Clearly, rescaling f does not change the value of R; therefore, without loss of generality we take $A=1$. Thus, if we expand the definition of R to lowest order in λ and use the above decomposition, we obtain

$$\sigma R=\frac{\left[\int f\Sigma_1 d\phi\right]^2}{\int f^2\Sigma_0 d\phi} \tag{15}$$

$$=\frac{\left[\int\frac{\Sigma_1^2}{\Sigma_0}d\phi\right]^2}{\int\frac{\Sigma_1^2}{\Sigma_0}d\phi+\int\hat{f}^2\Sigma_0 d\phi}\ . \tag{16}$$

Examining the denominator of Eq. (16), we note that if $\hat{f}$ is nonzero, the expression $\int\hat{f}^2\Sigma_0 d\phi$ is positive, and since the expression $\int\Sigma_1^2/\Sigma_0$ is also always positive, R is maximized when $\hat{f}=0$. R is therefore maximized when

$$f=f_{\rm opt}=\frac{\Sigma_1}{\Sigma_0}\ . \tag{17}$$

The preceding derivation of $f_{\rm opt}$ may also be understood in terms of the following argument. Let us consider the set of all functions of ϕ to be a vector space on which we define the scalar product

$$g_1\bullet g_2=\int g_1(\phi)g_2(\phi)\Sigma_0(\phi)d\phi\ , \tag{18}$$

where g_1 and g_2 are functions of ϕ. If we denote $f_0=\Sigma_1/\Sigma_0$, then in terms of this notation, Eq. (15) may be rewritten as

$$\sigma R=\frac{(f\bullet f_0)^2}{f\bullet f}\ . \tag{19}$$

From this formulation it is clear that R will be maximized when $f=f_0=f_{\rm opt}$, as we concluded above in Eq. (17).

As an illustrative example, consider a 2-to-2 scattering process where the differential cross section is of the form

$$\frac{d\sigma}{d\xi}=A+B\xi+C\xi^2\ , \tag{20}$$

where $\xi=\cos\theta$; $-1\le\xi\le+1$, and $B,C\le A$. According to the above recipe, if we wish a quantity which is most sensitive to B, we should take $f_B=\xi$, while the quantity most sensitive to C is $f_C=\xi^2$. Thus, we find

$$\sigma=2A+\tfrac{2}{3}C,\quad f_B^{(1)}(B)=\tfrac{2}{3}B,\quad f_B^{(2)}(B)=\tfrac{2}{3}A+\tfrac{2}{5}C\ ,$$
$$f_C^{(1)}(C)=\tfrac{2}{5}C+\tfrac{2}{3}A,\quad f_C^{(2)}(C)=\tfrac{2}{5}A+\tfrac{2}{7}C\ .$$

In the case of determining B the value of R (to lowest order in B and C) is thus given by

$$R(f_B)=\frac{1}{B^2}\frac{\left[\int_{-1}^{+1}B\xi^2 d\xi\right]^2}{\int_{-1}^{+1}A\,d\xi\int_{-1}^{+1}A\xi^2 d\xi}=\tfrac{1}{3}A^{-2}\ . \tag{21}$$

Likewise for C the value is $R(f_C)=\frac{1}{5}A^{-2}$.

One might also consider measuring B via another function which has the same symmetry properties as f_B. Consider, for example,

$$g_B(\xi)=\begin{cases}+1 & \text{if } \xi>0\ ,\\ -1 & \text{if } \xi<0\ .\end{cases} \tag{22}$$

In this case $g_B^{(1)}=B$ while $g_B^{(2)}=2A+\frac{2}{3}C$; hence, $R(g_B)=\frac{1}{4}A^{-2}$, which is less than the optimal value of $R(f_B)$.

Similarly, one might consider measuring C via the change in the total cross section, which is equivalent to using the function $g_C=1$. In this case $R(g_C)=\frac{1}{9}A^{-2}$, again less than the optimal value of $R(f_C)$.

In these cases, the difference between optimal and nonoptimal values of R is not that great; however, if there are a large number of degrees of freedom, more pronounced differences are possible.

Clearly, the $f_{\rm opt}$ inherits whatever discrete asymmetries Σ_1 has with respect to Σ_0. In the illustrative example f_B is antisymmetric under $\xi\leftrightarrow-\xi$ while f_C is symmetric under this symmetry. Likewise, in the case of observables sensitive to EDM and MDM couplings, the optimal observables will have the same transformation

properties under CP and P_n as the couplings. In particular, this prevents observables which are sensitive to one type of coupling from being sensitive to another coupling that has different symmetry properties [for example Re(C) versus Re(D)]. On the other hand, observables that are sensitive to a particular γ coupling will also be sensitive to the corresponding Z coupling [for example, the optimal observable for Re(C^γ) will also receive contributions from Re(C^Z)].

IV. MEASUREMENT OF DIPOLE MOMENTS

Consider now the process $e^+e^-\to t\bar{t}\to bW^+\bar{b}W^-$, where the W bosons subsequently undergo the decay $W\to l\nu_l$ ($l=e$, μ, or τ). The final state consists of the six particles $bl^+\nu_l\bar{b}l^-\bar{\nu}_l$. Of these one may only experimentally measure the momenta of the quarks and the leptons since the neutrinos escape detection. However, by imposing (1) conservation of four-momentum together with the conditions that (2) the lepton and neutrino reconstruct to the $W^\pm$ mass, (3) the b quark together with a lepton and neutrino reconstruct to the t, $\bar{t}$ mass, and (4) the neutrinos are massless, the momenta of the missing neutrinos may in fact be inferred. Furthermore, because of the left-handed nature of the coupling of the W boson to leptons, for $W\to l\nu_l$ the momenta of the decay products of the W boson determine the polarization of the W. Thus, in the W^- decay, $W^-(p_W)\to l^-(p_l)\bar{\nu}_l(p_\nu)$, the W polarization E^μ is given by the expression

$$E^\mu=\frac{\mathrm{Tr}[\not{p}_\nu\not{\omega}_0\not{p}_l\gamma^\mu(1-\gamma_5)]}{4\sqrt{p_\nu\cdot\omega_0 p_l\cdot\omega_0}}\ , \tag{23}$$

where ω_0 is an arbitrary lightlike vector that determines the phase convention for the polarization.

Under some conditions, it may not be possible to determine the polarization of the W boson. For example, if the W bosons were to decay into jets, the polarization would be undetermined unless the quark jet could be distinguished from the antiquark jet. We will therefore consider the measurement of EDM and MDM form factors both under conditions where the W polarizations may be determined and under conditions where they may not be.

Let us now turn our attention to the problem at hand and calculate the R value associated with the C_t and D_t couplings. For each coupling, we calculate the value of R and plot the quantity

$$\delta_n=\frac{1}{\sqrt{nR}}\frac{\sqrt{s}}{e}\ . \tag{24}$$

δ_n is thus the smallest value of the moment expressed in units of $e/\sqrt{s}$ which, given a sample of n events, may be detected with statistical significance $S=1$. Thus, for example, if $n=10\,000$ and $\sqrt{s}=500$ GeV then $\delta_{10\,000}=1$ implies that if the moment being considered has a value of $e/500$ GeV $=4\times10^{-17}$ e cm, it will produce a 1-σ effect given an experimental sample of 10 000 events observed.

Let us consider first MDM-type couplings which correspond to Re(C). In Fig. 2(a) we plot $\delta_{10\,000}$ as a function of $\sqrt{s}$ for $m_t=120$ GeV and unpolarized e^+e^- beams. The solid curve represents the value of $\delta_{10\,000}$ for a photon where the observable is the total cross section. In contrast the dashed curve represents the optimized observable. Clearly, in this case there is no great improvement. Likewise, the dotted line represents using the total cross section to determine Re(C_t^Z) while the dash-dot line represents the optimized observable for Re(C_t^Z). In this case the optimized observable gives a factor of about 4 increase in precision. In Fig. 2(b) we plot the same quantities for the case where both e^+ and e^- are right polarized, and in Fig. 2(c) we plot the same quantities in the case where the beams are left polarized. The right-polarized beams give the best results, which in the optimized case are about a factor of 2 better than the unpolarized case.

In Fig. 3(a) we consider operators which are sensitive to Im(C_t^γ) and $m_t=120$ GeV. The solid line represents $\delta_{10\,000}$ for the optimized observable where the beams are unpolarized; the long dash-dot curve is the case with left-polarized beams and the long dashed curve is the case with right-polarized beams. As before, the right-polarized beams give the best result, improving the precision by a factor of about 2. Also plotted are the optimized result for unpolarized beams and $m_t=160$ GeV (short dash-dot curve), which shows that there is not a great dependence of these results on m_t.

We have also considered what precision one can achieve if one neglects to measure the polarization of the W, for example, in the case where $W\to\bar{q}q'$ and one cannot identify the flavors of the quarks. The dotted curve in Figs. 3(a)–3(f) show $\delta_{10\,000}$ for the optimized observable which does not use the W polarization. As can be seen it is about a factor of 30 worse than what can be obtained using this polarization.

The optimized observable which we use above suffers from the fact that it is defined only through the relatively complicated equations given in the Appendix. It would also be desirable to consider an observable which, although not optimal, is of a simple form. Consider first the case of the imaginary MDM-type couplings [Im(C_t)]. In this case we have considered observables of the form

$$\epsilon_{\mu\nu\sigma\rho}k_1^\mu k_2^\nu k_3^\sigma k_4^\rho(k_5\cdot k_6)\ , \tag{25}$$

where

$$k_i\in\{P_t,Q_Z,P_e,P_b,Q_b,H^+,H^-\}\ , \tag{26}$$

which have the correct symmetry (even under CP, odd under P_n). The momenta mentioned above in the notation of the Appendix are

$$\begin{aligned}&P_t=\bar{p}_t-p_t,\quad Q_z=p_e^+ +p_e^-\ ,\\ &P_e=p_e^+ -p_e^-\ ,\\ &H^\pm=2E_W^+\cdot p_t\,E_W^+\pm2E_{\bar{W}}^-\cdot p_t\,E_{\bar{W}}^-\ .\end{aligned} \tag{27}$$

Of all the operators of the above type, it was found that the operator

$$\epsilon_{\mu\nu\sigma\rho}P_b^\mu Q_z^\nu H^{+\sigma}H^{-\rho}(P_b\cdot Q_z) \tag{28}$$

is the best in both the cases of Im(C_t^γ) and Im(C_t^Z). The

results for this operator are shown with the dashed curve in Fig. 3(a) for the case of $\mathrm{Im}(C_t^\gamma)$ and Fig. 3(b) for the case of $\mathrm{Im}(C_t^Z)$ assuming unpolarized e^+e^- beams. Note that this operator gives precision a factor of 5–10 poorer than the optimal operator.

In Fig. 3(c) we consider the measurement of the EDM, $\mathrm{Re}(D_t^\gamma)$. The curves we give are similar to those described above except that the form of the best simple operator indicated on the graph by the dashed line is

$$\epsilon_{\mu\nu\sigma\rho} P_b^\mu Q_z^\nu H^{+\sigma} H^{-\rho} . \tag{29}$$

Likewise, Fig. 3(d) shows a similar set of curves for the coupling $\mathrm{Re}(D_t^Z)$, where the best simple operator represented by the dashed curve is

$$\epsilon_{\mu\nu\sigma\rho} P_e^\mu Q_z^\nu H^{+\sigma} H^{-\rho} . \tag{30}$$

For the case of the imaginary EDM couplings, we have considered operators of either the form

$$(k_1 \cdot k_2)(k_3 \cdot k_4)$$

or

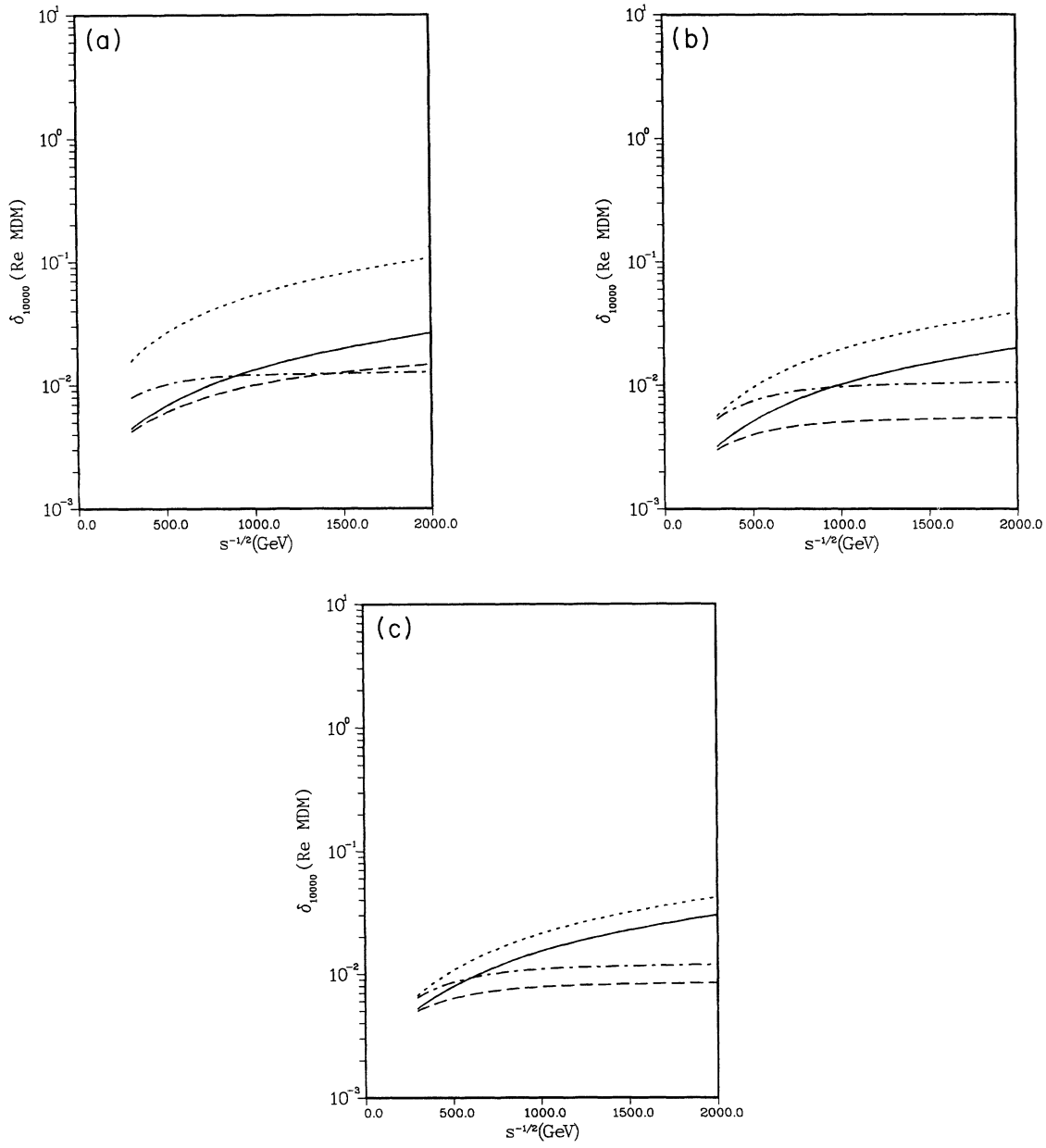

FIG. 2. $\delta_{10\,000}$ vs $\sqrt{s}$ is shown for various observables sensitive to $\mathrm{Re}(C)$. The curves shown are as follows: the dashed curve is $\delta_{10\,000}$ for the optimized observable for $\mathrm{Re}(C_t^\gamma)$; the solid curve is $\delta_{10\,000}$ using the total cross section to measure $\mathrm{Re}(C_t^\gamma)$; the dash-dot curve is $\delta_{10\,000}$ for the optimized observable for $\mathrm{Re}(C_t^Z)$; and the dotted curve is $\delta_{10\,000}$ using the total cross section to measure $\mathrm{Re}(C_t^Z)$. The polarization of the e^+e^- beams is taken to be unpolarized in (a), right polarized in (b), and left polarized in (c).

$$k_1 \cdot k_2 \ , \tag{31}$$

with the correct symmetry (CP odd, P_n even), k_i chosen as above. In both the γ and Z cases, the best operator of this form we found was

$$H^- \cdot Q_z \ . \tag{32}$$

In Figs. 3(e) and 3(f) we produce the corresponding dashed curves for the couplings $\mathrm{Im}(D_t^\gamma)$ and $\mathrm{Im}(D_t^Z)$, respectively.

From the above calculations we conclude that in the case of the real MDM couplings, $\mathrm{Re}(C_t)$, the use of an optimized operator instead of just looking at the change in the total cross section gives a factor of about 3 improvement in resolution, while using right-polarized beams gives another factor of about 3, giving a total gain using both improvements of about an order of magnitude. In the cases of $\mathrm{Im}(C_t)$, $\mathrm{Re}(D_t)$, and $\mathrm{Im}(D_t)$, we wish to

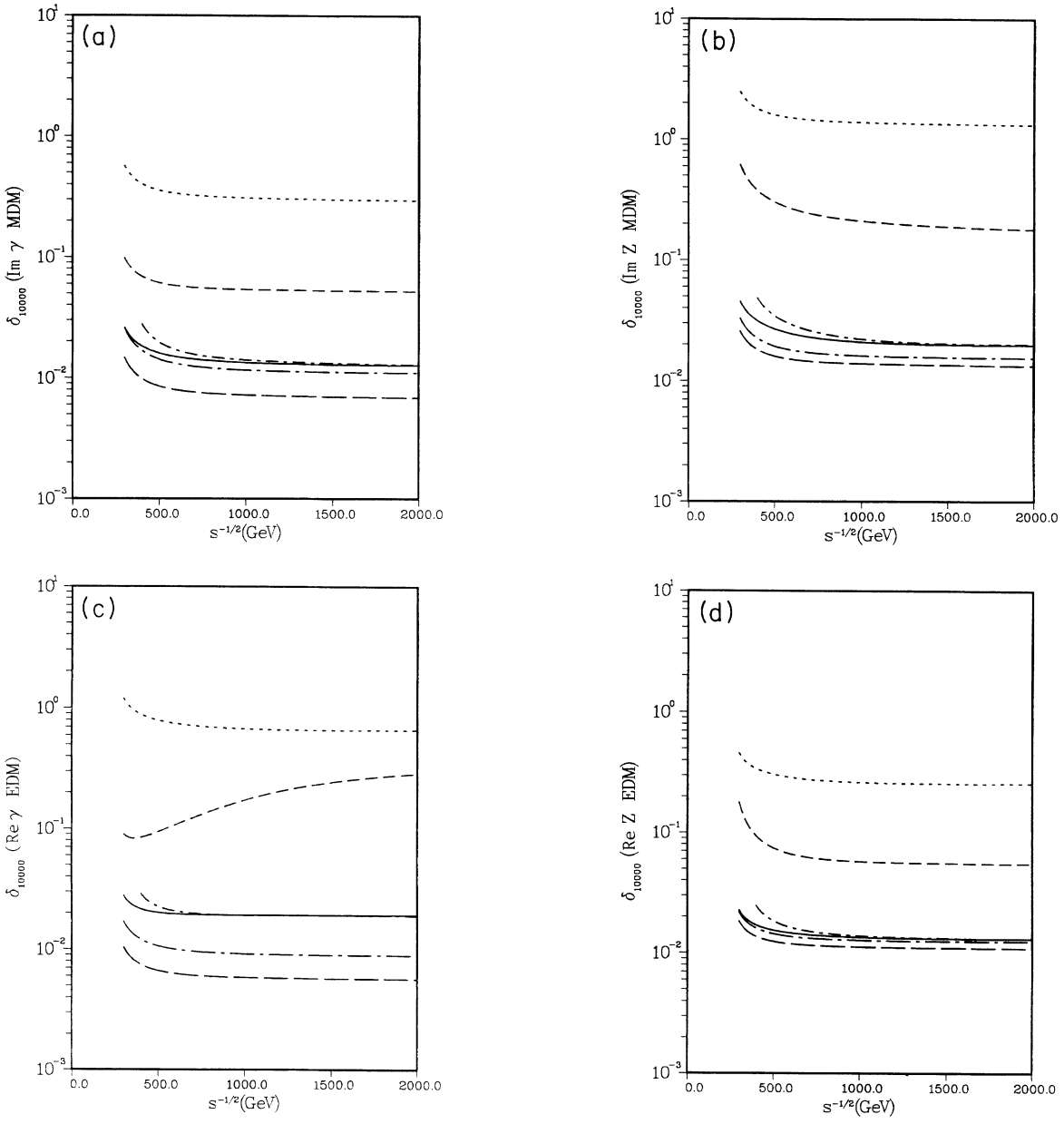

FIG. 3. Shown here is δ_{10000} vs $\sqrt{s}$ with respect to various couplings. The cases shown are (a) $\mathrm{Im}(C_t^\gamma)$; (b) $\mathrm{Im}(C_t^Z)$; (c) $\mathrm{Re}(D_t^\gamma)$; (d) $\mathrm{Re}(D_t^Z)$; (e) $\mathrm{Im}(D_t^\gamma)$; and (f) $\mathrm{Im}(D_t^Z)$. In each case the optimal observable for unpolarized beams using $m_t = 120$ GeV is shown with the solid curve; the optimal with left-polarized beams is shown with the long dash-dot curve; the optimal with right-polarized beams is shown with the long dash curve. The optimal curve using unpolarized beams and $m_t = 160$ GeV is shown with the short dash-dot curve; the optimal case where W-boson polarization is not measured is shown with the dotted curve. The best that can be achieved with the simple operators described in the text is shown with the dashed curve.

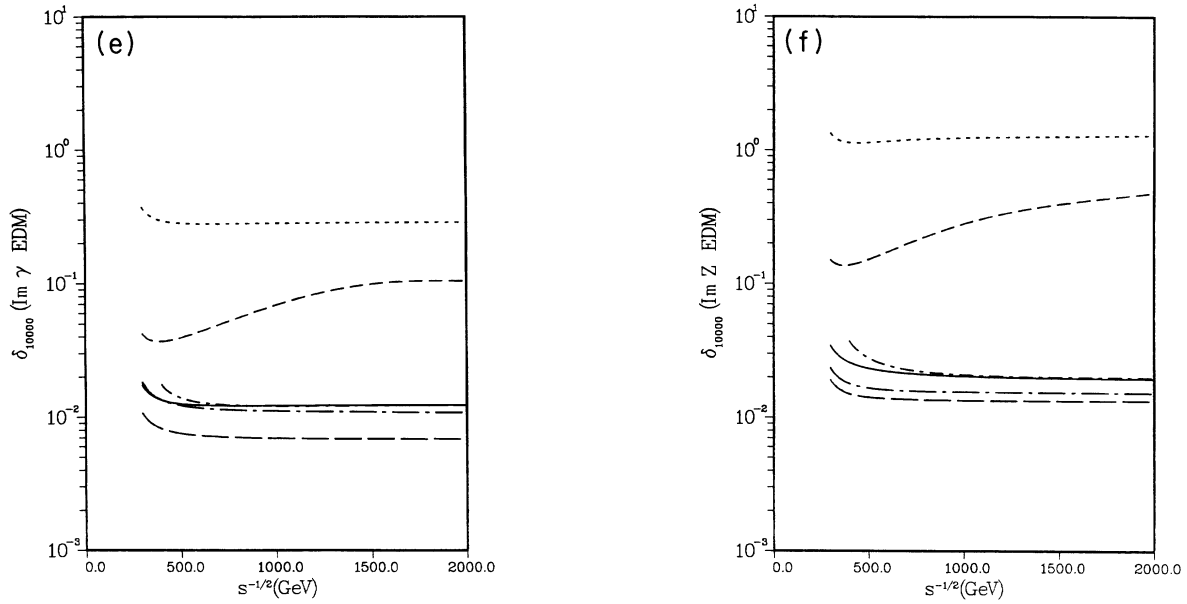

FIG. 3. (*Continued*).

emphasize that a simple operator constructed using the W-boson polarizations gives an improvement of an order of magnitude over what can be done without using that information, and an additional factor of 5–10 improvement is obtained by considering the optimal observable. If, in addition, one is able to use polarized beams, some further improvement occurs, the best case being with right polarized beams where an additional factor of about 2 is obtained. The graphs in these three cases tend to be constant as $\sqrt{s}$ increases; hence, the value of the moment one can measure improves linearly with $\sqrt{s}$. The resolution, however, deteriorated near threshold. In contrast, in the case of Re(C_t) the resolution does not deteriorate near threshold.

ACKNOWLEDGMENTS

We would like to gratefully acknowledge helpful discussions with Michael Peskin [6]. This work was supported by the U.S. Department of Energy under Contract No. DE-AC02-76CH00016, and the work of D.A. was partially supported by the Natural Sciences and Engineering Council of Canada.

APPENDIX

The basic four-vectors we shall use are $p_e^{\pm}$ which is the four-momentum of the $e^{\pm}$, p_b, which is the four-momentum of the b quark, $\bar{p}_b$, which is the four-momentum of the $\bar{b}$ quark, p_t, which is the four-momentum of the t quark, $\bar{p}_t$, which is the four-momentum of the $\bar{t}$ quark, and $E_W^{\pm}$, which is the polarization of the $W^{\pm}$.

We also define the following kinematic angles: θ_t is the angle between the top quark and the electron three-momentum in the center-of-mass frame, and ϕ_t is the azimuthal angle of the top quark three-momentum about the electron-beam axis. θ_b and ϕ_b are the angles of the b quark in the rest frame of the t quark. Likewise, $\theta_{\bar{b}}$ and $\phi_{\bar{b}}$ are the angles of the b quark in the rest frame of the $\bar{t}$ quark. We express our phase space in terms of these angles as

$$d\phi=\frac{1}{(4\pi)^3}d\cos\theta_t d\phi_t d\cos\theta_b d\phi_b d\cos\theta_{\bar{b}} d\phi_{\bar{b}} \ . \quad \text{(A1)}$$

Below we will calculate the differential cross section $\Sigma(\phi)d\phi$ for the process $e^+e^-\to t\bar{t}\to bW^+\bar{b}W^-$ to first order in C_t and D_t. We decompose Σ as

$$\Sigma d\phi=(\Sigma_{AB}+\Sigma_{\mathrm{Re}(C)}+\Sigma_{\mathrm{Im}(C)}+\Sigma_{\mathrm{Re}(D)}+\Sigma_{\mathrm{Im}(D)})d\phi \ , \quad \text{(A2)}$$

where Σ_{AB} is independent of C_t and D_t, $\Sigma_{\mathrm{Re}(C)}$ is proportional to Re(C), $\Sigma_{\mathrm{Im}(C)}$ is proportional to Im(C), $\Sigma_{\mathrm{Re}(D)}$ is proportional to Re(D), and $\Sigma_{\mathrm{Im}(D)}$ is proportional to Im(D).

For the purposes of our calculation, let us combine the four-momenta of the particles as follows:

$$\begin{aligned}
&P_t=\bar{p}_t-p_t, \quad Q_z=p_e^+ +p_e^- \ , \\
&P_e=p_e^+ -p_e^- \ , \\
&p_B=p_b+2E_W^+\cdot p_t\, E_W^+, \quad \bar{p}_B=\bar{p}_b+2E_W^-\cdot\bar{p}_t\, E_W^- \ , \quad \text{(A3)} \\
&F_B=p_B-\frac{p_B\cdot p_t}{m_t^2}p_t, \quad \bar{F}_B=\bar{p}_B-\frac{\bar{p}_B\cdot\bar{p}_t}{m_t^2}\bar{p}_t \ , \\
&Q_F=\bar{F}_B+F_B, \quad P_F=\bar{F}_B-F_B \ ,
\end{aligned}$$

in terms of which we define the quantities

$$\begin{aligned}
&s=Q_Z^2, \quad x_t=\frac{m_t^2}{s}, \quad x_W=\frac{m_W^2}{s}, \quad u_t=\frac{p_e\cdot p_t}{s} \ , \\
&u_F=\frac{Q_F\cdot Q_Z}{s}, \ v_F=\frac{Q_F\cdot P_t}{s}, \quad u_G=\frac{P_F\cdot P_e}{s}, \quad v_G=\frac{Q_F\cdot P_e}{s} \ ,
\end{aligned} \quad \text{(A4)}$$

$$x_F=\frac{Q_F^2}{s},\quad y_F=\frac{P_F^2}{s},\quad R^{\pm}=\frac{1}{m_t^2}(\bar{p}_B\cdot\bar{p}_t\pm p_B\cdot p_t)\ ,$$

$$\epsilon_3=\frac{1}{s^2}\epsilon_{\mu\nu\sigma\rho}P_t^{\mu}Q_Z^{\nu}P_e^{\sigma}Q_F^{\rho},\quad \epsilon_4=\frac{1}{s^2}\epsilon_{\mu\nu\sigma\rho}P_t^{\mu}Q_Z^{\nu}P_e^{\sigma}P_F^{\rho}\ .$$

We give here the following formulas for the differential cross section in two cases: unpolarized e^+e^- beams and the exchange of only one vector meson (e.g., exchange of only the Z boson), and longitudinally polarized e^+e^- beams with multiple-vector exchange (in particular, if one boson is the Z and the other the γ we have the case for which we calculate numerical results). Both cases may be derived from the expressions below by the following assignments to the parameters a_k, c_k, and d_k, which will then be substituted into Eq. (A8) to obtain the differential cross section.

First of all, in the case of single-vector exchange with unpolarized beams let us define $f=(A_e^2+B_e^2)$, $g=2A_eB_e$, and $r_V=s/(s-m_V^2)$. We then assign the parameters a_k, c_k, and d_k according to the expressions

$$\begin{aligned}
&a_1=fA_t^2r_V^2,\quad a_2=fB_t^2r_V^2\ ,\\
&a_3=2fA_tB_tr_V^2,\quad a_4=gA_t^2r_V^2\ ,\\
&a_5=gB_t^2r_V^2,\quad a_6=2gA_tB_tr_V^2\ ,\\
&c_1^{\rm re}=f\,{\rm Re}(A_tC_t)r_V^2,\quad c_2^{\rm re}=f\,{\rm Re}(B_tC_t)r_V^2\ ,\\
&c_3^{\rm re}=g\,{\rm Re}(A_tC_t)r_V^2,\quad c_4^{\rm re}=g\,{\rm Re}(B_tC_t)r_V^2\ ,\\
&c_1^{\rm im}=f\,{\rm Im}(A_tC_t)r_V^2,\quad c_2^{\rm im}=f\,{\rm Im}(B_tC_t)r_V^2\ ,\\
&c_3^{\rm im}=g\,{\rm Im}(A_tC_t)r_V^2,\quad c_4^{\rm im}=g\,{\rm Im}(B_tC_t)r_V^2\ ,\\
&d_1^{\rm re}=f\,{\rm Re}(A_tD_t)r_V^2,\quad d_2^{\rm re}=f\,{\rm Re}(B_tD_t)r_V^2\ ,\\
&d_3^{\rm re}=g\,{\rm Re}(A_tD_t)r_V^2,\quad d_4^{\rm re}=g\,{\rm Re}(B_tD_t)r_V^2\ ,\\
&d_1^{\rm im}=f\,{\rm Im}(A_tD_t)r_V^2,\quad d_2^{\rm im}=f\,{\rm Im}(B_tD_t)r_V^2\ ,\\
&d_3^{\rm im}=g\,{\rm Im}(A_tD_t)r_V^2,\quad d_4^{\rm im}=g\,{\rm Im}(B_tD_t)r_V^2\ .
\end{aligned}\tag{A5}$$

In the case of longitudinal-polarized beams with multiple-vector exchange, let us denote the helicity of the $e^{\pm}$ by $h_{\pm}$. Thus the $e^{\pm}$ beam contains a proportion of $\frac{1}{2}(1+h_{\pm})$ right-handed particles and $\frac{1}{2}(1-h_{\pm})$ left-handed particles. We further define the quantities $\alpha=1+h_+h_-$ and $\beta=h_++h_-$. For each pair of vector bosons V_i and V_j let us define

$$\begin{aligned}
f_{ij}&=[\alpha(A_e^iA_e^j+B_e^iB_e^j)+\beta(A_e^iB_e^j+B_e^iA_e^j)]r_ir_j\ ,\\
g_{ij}&=[\beta(A_e^iA_e^j+B_e^iB_e^j)+\alpha(A_e^iB_e^j+B_e^iA_e^j)]r_ir_j\ ,
\end{aligned}\tag{A6}$$

where $r_i=s/(s-m_i^2)$. Using these definitions, values of the parameters a_k, c_k, and d_k are

$$\begin{aligned}
&a_1=\sum_{ij}f_{ij}A_t^iA_t^j,\quad a_2=\sum_{ij}f_{ij}B_t^iB_t^j\ ,\\
&a_3=\sum_{ij}f_{ij}(A_t^iB_t^j+B_t^iA_t^j),\quad a_4=\sum_{ij}g_{ij}A_t^iA_t^j\ ,\\
&a_5=\sum_{ij}g_{ij}B_t^iB_t^j,\quad a_6=\sum_{ij}g_{ij}(A_t^iB_t^j+B_t^iA_t^j)\ ,\\
&c_1^{\rm re}=\sum_{ij}f_{ij}A_t^j{\rm Re}(C_t^i),\quad c_2^{\rm re}=\sum_{ij}f_{ij}B_t^j{\rm Re}(C_t^i)\ ,\\
&c_3^{\rm re}=\sum_{ij}g_{ij}A_t^j{\rm Re}(C_t^i),\quad c_4^{\rm re}=\sum_{ij}g_{ij}B_t^j{\rm Re}(C_t^i)\ ,\\
&c_1^{\rm im}=\sum_{ij}f_{ij}A_t^j{\rm Im}(C_t^i),\quad c_2^{\rm im}=\sum_{ij}f_{ij}B_t^j{\rm Im}(C_t^i)\ ,\\
&c_3^{\rm im}=\sum_{ij}g_{ij}A_t^j{\rm Im}(C_t^i),\quad c_4^{\rm im}=\sum_{ij}g_{ij}B_t^j{\rm Im}(C_t^i)\ ,\\
&d_1^{\rm re}=\sum_{ij}f_{ij}A_t^j{\rm Re}(D_t^i),\quad d_2^{\rm re}=\sum_{ij}f_{ij}B_t^j{\rm Re}(D_t^i)\ ,\\
&d_3^{\rm re}=\sum_{ij}g_{ij}A_t^j{\rm Re}(D_t^i),\quad d_4^{\rm re}=\sum_{ij}g_{ij}B_t^j{\rm Re}(D_t^i)\ ,\\
&d_1^{\rm im}=\sum_{ij}f_{ij}A_t^j{\rm Im}(D_t^i),\quad d_2^{\rm im}=\sum_{ij}f_{ij}B_t^j{\rm Im}(D_t^i)\ ,\\
&d_3^{\rm im}=\sum_{ij}g_{ij}A_t^j{\rm Im}(D_t^i),\quad d_4^{\rm im}=\sum_{ij}g_{ij}B_t^j{\rm Im}(D_t^i)\ .
\end{aligned}\tag{A7}$$

The terms in the partial cross section expansion are thus

$$\begin{aligned}
\Sigma_{AB}&=N[a_1(U_1+U_1')+a_2(U_2+U_2')\\
&\quad+a_3U_3+a_4U_4+a_5U_5+a_6U_6]\ ,\\
\Sigma_{{\rm Re}(C)}&=N'(c_1^{\rm re}X_C^1+c_2^{\rm re}X_C^2+c_3^{\rm re}X_C^3+c_4^{\rm re}X_C^4)\ ,\\
\Sigma_{{\rm Im}(C)}&=N'(c_1^{\rm im}Y_C^1+c_2^{\rm im}Y_C^2+c_3^{\rm im}Y_C^3+c_4^{\rm im}Y_C^4)\ ,\\
\Sigma_{{\rm Re}(D)}&=N'(d_1^{\rm re}X_D^1+d_2^{\rm re}X_D^2+d_3^{\rm re}X_D^3+d_4^{\rm re}X_D^4)\ ,\\
\Sigma_{{\rm Re}(D)}&=N'(d_1^{\rm im}Y_D^1+d_2^{\rm im}Y_D^2+d_3^{\rm im}Y_D^3+d_4^{\rm im}Y_D^4)\ .
\end{aligned}\tag{A8}$$

The normalization constants N, N' are given by

$$\begin{aligned}
N&=\frac{\sqrt{1-4x_t}}{\pi s}\frac{x_W^2x_t}{(x_t-x_W)^2(x_t+2x_W)^2}\ ,\\
N'&=m_tN\ .
\end{aligned}\tag{A9}$$

The quantities U_i, X_C^i, Y_C^i, X_D^i, and Y_D^i are given by the expressions

$$
\begin{aligned}
U_1 &= \frac{-x_t}{16}[(R^-)^2-(R^+)^2](u_t^2+4x_t+1)\ , \\
U_1' &= -\tfrac{1}{16}[(x_F-y_F)(1-4x_t-u_t^2)+2(v_G^2+v_F^2-u_G^2-u_F^2) \\
&\quad +4u_t(v_Gv_F+u_Gu_F)]\ , \\
U_2 &= \frac{-x_t}{16}[(R^-)^2-(R^+)^2](u_t^2-4x_t+1)\ , \\
U_2' &= \tfrac{1}{16}[(x_F-y_F)(1-4x_t-u_t^2) \\
&\quad +2(1-4x_t)(v_G^2+v_F^2-u_G^2-u_F^2) \\
&\quad +4u_t(v_Gv_F+u_Gu_F)]\ , \\
U_3 &= \frac{-x_t}{4}[R^-(v_Gu_t-v_F)-R^+(u_Gu_t+u_F)]\ , \\
U_4 &= \frac{x_t}{2}(R^-v_G-R^+u_G)\ , \\
U_5 &= \frac{-x_tu_t}{2}(R^-v_F+R^+u_F)\ , \\
U_6 &= \frac{x_t}{8}\{u_t[(R^-)^2-(R^+)^2]-4(v_Fv_G+u_Fu_G)\}\ ,
\end{aligned}
\tag{A10}
$$

$$
\begin{aligned}
X_C^1 &= \tfrac{1}{2}\{x_t[(R^-)^2-(R^+)^2]+v_G^2-u_G^2 \\
&\quad +u_t(v_Fv_G+u_Fu_G)\}\ , \\
X_C^2 &= \tfrac{1}{4}\{R^-[v_Gu_t+v_F(u_t^2-4x_t)] \\
&\quad -R^+[u_Gu_t-u_F(u_t^2-4x_t)]\}\ , \\
X_C^3 &= -\tfrac{1}{4}\{R^-[v_Fu_t+v_G(1+4x_t)] \\
&\quad +R^+[u_Fu_T-u_G(1+4x_t)]\}\ , \\
X_C^4 &= -\tfrac{1}{2}\{x_tu_t[(R^-)^2-(R^+)^2]+u_t(u_F^2-v_F^2) \\
&\quad -(u_Fu_G+v_Fv_G)\}\ , \\
Y_C^1 &= \frac{u_t}{4}(R^+\epsilon_4-R^-\epsilon_3)\ , \\
Y_C^2 &= \tfrac{1}{2}(u_G\epsilon_4-v_G\epsilon_3)\ , \\
Y_C^3 &= -\tfrac{1}{2}(u_F\epsilon_4+v_F\epsilon_3)\ , \\
Y_C^4 &= -\tfrac{1}{4}(R^+\epsilon_4-R^-\epsilon_3)\ , \\
X_D^1 &= -\tfrac{1}{2}(v_G\epsilon_4-u_G\epsilon_3)\ , \\
X_D^2 &= -\frac{u_t}{4}(R^-\epsilon_4-R^+\epsilon_3)\ , \\
X_D^3 &= \tfrac{1}{4}(R^-\epsilon_4-R^+\epsilon_3)\ , \\
X_D^4 &= -\tfrac{1}{2}(v_F\epsilon_4+u_F\epsilon_3)\ , \\
Y_D^1 &= -\tfrac{1}{4}\{R^-[u_Gu_t-(u_t^2+4x_t)u_F] \\
&\quad -R^+[v_Gu_t+(u_t^2+4x_t)v_F]\}\ , \\
Y_D^2 &= \frac{u_t}{2}(v_Gu_F+u_Gv_F)\ , \\
Y_D^3 &= -\tfrac{1}{2}(v_Gu_F+u_Gv_F)\ , \\
Y_D^4 &= -\tfrac{1}{4}\{R^-[u_Fu_t-(1-4x_t)u_G] \\
&\quad +R^+[v_Fu_t+(1-4x_t)v_G]\}\ .
\end{aligned}
\tag{A11, A12}
$$

[1] CDF Collaboration, L. Pondrom, in *Proceedings of the 25th International Conference on High Energy Physics,* Singapore, 1990, edited by K. K. Phua and Y. Yamaguchi (World Scientific, Singapore, 1991).

[2] See, for example, Burton Richter, in *Proceedings of the 24th International Conference on High Energy Physics,* Munich, West Germany, 1988, edited by R. Kotthaus and J. Kuhn (Springer, Berlin, 1988).

[3] For a demonstration that the neutron does not receive an EDM at ≤ 2 loops in the standard model, see E. P. Shabalin, Yad. Fiz. **31**, 1665 (1980) [Sov. J. Nucl. Phys. **31**, 864 (1980)]; **32**, 443 (1980) [**32**, 228 (1980)]. For an example of a three-loop graph that produces a fermion EDM in the standard model, see F. Hoogeveen, Nucl. Phys. **B341**, 322 (1990).

[4] A. Pich and E. de Rafael, Nucl. Phys. **B367**, 313 (1991), and references therein; R. J. Crewther, P. Di Vecchia, G. Veneziano, and E. Witten, Phys. Lett. **88B**, 123 (1979); G. 't Hooft, Phys. Rev. Lett. **37**, 8 (1976).

[5] For a review of fermion EDM's generated by various models, see W. Marciano, in *Proceedings of the Summer Study on CP Violation,* Upton, New York, 1990, edited by S. Dawson and A. Soni (World Scientific, Singapore, 1990); S. Barr and W. Marciano, in *CP Violation,* edited by C. Jarlskog (World Scientific, Singapore, 1989), p. 455; W. Bernreuther and M. Suzuki, Rev. Mod. Phys. **63**, 313 (1991); W. Grimus, in Proceedings of Topical Meeting on *CP* Violation, Calcutta, India, 1990 (unpublished); N. F. Ramsey, Annu. Rev. Nucl. Part. Sci. **32**, 211 (1982).

[6] In particular, we want to thank Michael Peskin for informing us of two related works: G. L. Kane, G. A. Ladinsky, and C. P. Yuan, Phys. Rev. D **45**, 124 (1992); M. E. Peskin and M. J. Strassler (in preparation).